

Analyst

Accepted Manuscript



This is an *Accepted Manuscript*, which has been through the Royal Society of Chemistry peer review process and has been accepted for publication.

Accepted Manuscripts are published online shortly after acceptance, before technical editing, formatting and proof reading. Using this free service, authors can make their results available to the community, in citable form, before we publish the edited article. We will replace this *Accepted Manuscript* with the edited and formatted *Advance Article* as soon as it is available.

You can find more information about *Accepted Manuscripts* in the [Information for Authors](#).

Please note that technical editing may introduce minor changes to the text and/or graphics, which may alter content. The journal's standard [Terms & Conditions](#) and the [Ethical guidelines](#) still apply. In no event shall the Royal Society of Chemistry be held responsible for any errors or omissions in this *Accepted Manuscript* or any consequences arising from the use of any information it contains.



Analyst

Paper

Benzindole substituted carbazole cyanine dye: a novel targeting fluorescent probe for parallel c-myc G-Quadruplex

Dayong Lin^a, Xuening Fei^{*a,b}, Yingchun Gu^{*b,c}, Cuihong Wang^b, Yalin Tang^{c*}, Ran Li^b and Jianguo Zhou^b

Received 00th January 20xx,
Accepted 00th January 20xx

DOI: 10.1039/x0xx00000x

www.rsc.org/

Many organic ligands were synthesized to recognize G-quadruplex. However, different kinds of G-quadruplexes (G4s) possess different structures and functions. Therefore, selective recognition of certain types of G4s is important for the study of G4s. In this paper, a novel cyanine dye, 3-(2-(4-vinylpyridine))-6-(2-((1-(4-Sufobutyl))-3,3-dimethyl-2-vinylbenz[e]indole)-9-ethyl)-carbazole (9E PBIC) composed of benzindole and carbazole was designed and synthesis. The studies on UV-vis and fluorescent properties between the dye with different DNA showed that the dye exhibits almost no fluorescence in the aqueous buffer condition, but increased over 100 fold in the presence of c-myc G4 and 10-30 fold in the presence of other G4s, while little in the presence of single/double-stranded DNA, which indicating that it is of excellent selectivity to c-myc 2345 G4. The binding studies indicate that the dye is interacted with c-myc 2345G-quadruplex by end-stack binding model. It is said that the dye is of an excellent targeting fluorescent probe for c-myc G-quadruplex.

Introduction

G-quadruplexes (G4s) are four-stranded DNA helical secondary structures folded by G-rich sequences.¹⁻² A variety of G-rich sequences are found in locations widely prevalent at eukaryotic telomeres in the human genome, in proliferation, in RNA sequences and in oncogenes promoters. Oncogenes with promoter sequences that in vivo have been shown to form stable G4 arrangements include bcl-2, c-kit, c-myc, KRAS, BRAF, SRC and so on.³⁻¹⁰ Because of its formation mostly related to the processes of transcription, replication, and recombination, it is highly associated with human diseases¹¹ (e.g., cancer,^{12,13} cardiovascular diseases¹⁴ and diabetes¹⁵). The recognition of G-quadruplex is very important and significance in both biology and supramolecular chemistry.¹⁶⁻¹⁸ Many G4 ligands have been designed and synthesized, which contain a planar aromatic core that bind to G4s through π - π stacking interactions and exhibit absorption or fluorescence. But few molecules in the reported G4 ligand show a high selectivity or specific for G4s over duplex DNA, especially specifically recognized G4s with specific structures.¹⁹⁻³¹

The c-myc gene promoter G4 structure was selected as the target in view of its important role linked to human cancers,

such as breast cancer, cervical cancer, leukemia, et al. with the additional advantage that it adopts only one conformation, a propeller-type parallel-stranded G4s.³²⁻³⁴ Therefore, the selectivity for G4s over duplex DNA, especially specificity and selectivity recognizing for G4s with specific structure is crucial for small molecules to be promising G-quadruplex probes.³⁵⁻³⁸ Up to now, carbazole and its derivatives have been widely utilized as a functional building block in the fabrication of the organic medicine, pesticide, material, etc., because of their excellent solubility, stability, large π -conjugation system, special rigid structure, easily functionalized at 3, 6 and 9-positions and covalently linked with other molecular groups, excellent and biological activity. In addition, carbazole and its derivatives can be used as a strong electro-donating chromophore, which is the main structure of fluorescent dyes. As the intramolecular charge transfer (ICT) exists in the D-A molecules of carbazole, many carbazole derivatives offer large Stokes shifts and high quantum yields³⁹⁻⁴³. For example, small molecule, 3, 6-Bis(1-methyl-4-vinylpyridinium) carbazole diiodide (BMVC) and its derivatives are not only G4 stabilizers⁴⁴, but also fluorescence probes with higher binding affinity to quadruplex than to duplex DNA.^{45,46} They show a significant fluorescence enhancement in the presence of DNA and a higher sensitivity and binding preference to some G4s. Also, BPBC⁴⁷ as well as dimeric carbazole-benzimidazole for stabilization G-quadruplex DNA were reported⁴⁸.

However, the fluorescent emission maximum wavelength for BMVC is at 575nm and for BPBC and dimeric carbazole-benzimidazole are only about 460 nm, which were very close to those of organisms and may be resulting in error and mistake when it was used as a biomarker. It is highly desirable

^aSchool of Environmental Science and Engineering, Tianjin University, Tianjin, 300072, China. E-mail: xueningfei@126.com

^bSchool of Science, Tianjin Chengjian University, Tianjin, 300384, China. E-mail: jvgugugu@126.com

^cInstitute of Chemistry, Chinese Academy of Sciences (ICCAS), Beijing, 100190, China. E-mail: tangyl@iccas.ac.cn

† Electronic Supplementary Information (ESI) available. See DOI: 10.1039/x0xx00000x

to develop long wavelength (red to near infrared) G-quadruplex-responsive fluorescent probes⁴⁹ with various advantages, including minimum photo-damage to biological samples, diminishing Rayleigh–Tyndall scattering of light, deep tissue penetration and minimum autofluorescence.⁵⁰ Some cyanine dye also can recognize G4s from other DNA sequences with longer wavelength, such as benzothiazole-substituted benzofuroquinolinium dye⁵¹, Halogenated pentamethine cyanine dyes⁵², [2.2.2]-heptamethinecyanine dye.^{53–55} TSQ1 can be a optical dye probe for all G4⁵⁶ with poor selectivity and 5 to 70 folds fluorescence enhancements binding to G4s.

In order to enhance the good selectivity toward specific G4s of the carbazole derivatives and cyanine dyes, we attempted to assemble BMVC and benzindole in a fusion scaffold. By fusing a fluorophore, benzindole ring is introduced to replace one pyridine ring of 9E-BMVC, a novel molecule, 3-(2-(4-vinylpyridine))-6-(2-((1-(4-Sufobutyl))-3,3-dimethyl-2-vinylbenz[e]indole)-9-ethyl-carbazole (9E PBIC) was firstly designed and synthesized (Fig. 1), aiming to optimize its photophysical property (Table S1) and selectivity for G4 through its expanded π -conjugated aromatic system. The novel dye has almost no fluorescence in aqueous solution but exhibits a fluorescence enhancement upon binding to G4s, especially the parallel c-myc 2345 G4. The optical properties of the dye upon binding to different DNA were investigated and the interaction mechanism was discussed.

Experimental section

Materials and Reagents

9-ethyl-9H-carbazole and N-bromosuccinimide (NBS) were purchased from Sinopharm Chemical Reagent Co. Ltd (Shanghai, China). Palladium (II) acetate, 4-vinylpyridine and tri-*o*-tolylphosphine were purchased from Energy Chemical. The thin layer chromatography (TLC) analyses were performed on silica gel plates and column chromatography was conducted over silica gel (mesh 200–300), both of which were obtained from Qingdao Ocean Chemicals. All ordinary solvents and chemical reagents were used as received without further purification.

Synthesis of the cyanine dye

The synthesis procedures of compound 1 and 2 were based on the references.^{57, 58} The synthesis procedure of compound 4 was based on the Ref.⁵⁹

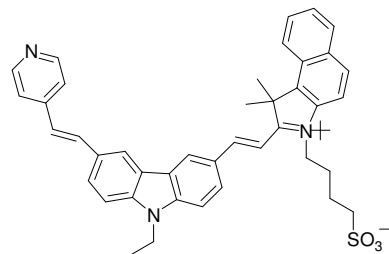
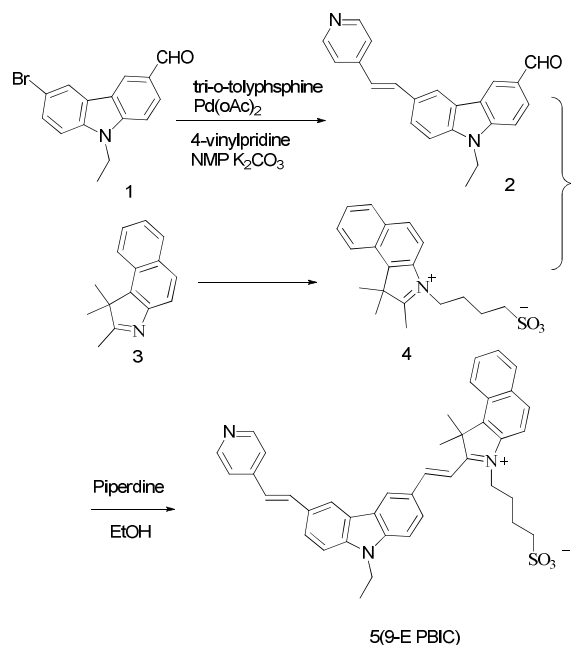


Fig. 1 The molecular structures of dye

Compound 2 ¹H NMR (400 MHz, CDCl₃): δ 1.52 (J = 6.8 Hz, 3H), 4.44–4.47 (m, 2H), 7.11 (d, J = 20.4 Hz, 1H), 7.47–7.57 (m, 4H), 7.78 (d, J = 8.4 Hz, 1H), 8.06 (d, J = 8.0 Hz, 1H), 8.35 (s, 1H), 8.65 (d, J = 15.6 Hz, 3H), 10.14 (s, 1H).

Synthesis of 3-(4-vinylpyridine)-6-(3-(4-Sufobutyl)-1,1-dimethyl-2-vinylbenz[e]indole)-9-ethyl-carbazole (9E PBIC) (Scheme 1)

Compound 4 (1 mmol) and compound 2 (1.1 mmol) were added to a 50 mL flask with ethanol (25 mL), followed by catalytic piperidine (0.10 mL). The resulting mixture was allowed to stir about 4 h and monitored by TLC (dichloromethane–methanol, 6:1). The solvent was removed under reduced pressure and the crude mixture was purified on silica using dichloromethane/methanol 10:1 as an eluent to afford the product as brownish red solid. Yield: 65%. Purity: 98.6% (HPLC). ¹H NMR (400 MHz, DMSO-*d*₆): δ 1.39–1.43 (t, J = 7.2 Hz, 3H), 2.03–2.08 (m, 2H), 2.10 (s, 6H), 2.20–2.23 (m, 2H), 2.84–2.87 (t, J = 6.2 Hz, 2H), 4.53–4.58 (m, 2H), 4.84–4.88 (m, 2H), 7.67 (d, J = 5.6 Hz, 2H), 7.70–7.78 (m, 4H), 7.80–7.83 (t, J = 6.8 Hz, 3H), 8.07 (d, J = 16 Hz, 1H), 8.16 (d, J = 9.2 Hz, 1H), 8.22 (d, J = 8.0 Hz, 1H), 8.28–8.31 (m, 2H), 8.44 (d, J = 8.4 Hz, 1H), 8.55 (d, J = 5.6 Hz, 2H), 8.75 (d, J = 16 Hz, 1H), 8.96 (s, 1H), 9.65 (s, 1H). ¹³C NMR (400 MHz, DMSO-*d*₆): δ 182.18, 170.81, 155.2, 150.0, 145.9, 144.0, 141.2, 138.9, 138.2, 134.0, 133.4, 131.4, 130.5, 129.7, 128.8, 127.8, 127.3, 126.9, 124.7, 124.3, 124.0, 123.8, 123.4, 121.3, 113.4, 110.6, 110.4, 109.3, 60.3, 53.7, 49.7, 46.7, 44.2, 26.5, 24.2, 22.7, 22.6, 22.1, 21.3, 14.6, 14.4. MS (TOF): calcd for C₄₁H₃₉N₃O₃SN⁺ (M +Na⁺) m/z 676.2610, found 676.6491.



Scheme 1 synthesis route of the dye

Oligonucleotides

All oligonucleotides were purchased from Invitrogen Co. (Beijing, China). d24 (dsDNA) was prepared by heat denaturing and annealing the mixture of A24 and s24 (1:1).

The stock solution of 9E PBIC (100 μM) was prepared by dissolving it into DMSO and stored in the dark at room temperature.

The stock solutions of oligonucleotides were prepared by dissolving them in Tris-HCl buffer (10 mM Tris-HCl, pH = 7.4), Na^+ buffer (10 mM Tris-HCl, 100 mM NaCl, 0.1 mM EDTA, pH = 7.4) or K^+ buffer (10 mM Tris-HCl, 20 mM KCl, 0.1 mM EDTA, pH = 7.4). The concentration of oligonucleotides was determined based on their absorbance at 260 nm. The measured samples were prepared by adding different concentrations of the corresponding DNA stock solutions into Tris- K^+ or Tris- Na^+ buffer containing 6 μM dye, respectively. The samples were incubated overnight in the dark at room temperature before their use for testing.

Absorption and fluorescence measurements

The absorbance spectra were recorded on a UV-1900 (Beijing Purkinje General Instrument Co. Ltd.) instrument. Fluorescence spectra were recorded on a Hitachi F-7000 fluorescence spectrophotometer (Kyoto, Japan). The excitation wavelength was 530 nm. The slit width of both excitation and emission were 5 nm, and the voltage was set to 700 V with a scan speed of 1200 nm min^{-1} . DNA titration experiment: concentration of 9E PBIC was fixed at 6 μM , and the final concentration of DNA was 0, 1.5, 3, 6, 9, 12, 15, 18 μM , spectra were recorded after standing overnight at room temperature. Final analysis of the data was carried out using Origin 8.0 (OriginLab Corp.).

Circular dichroism Spectroscopy

CD spectra were recorded on a MOS-450 spectrometer (Biologic in French) in the wavelength range of 200–450 nm using a 1 mm pathlength quartz cuvette. The scanning speed of the instrument was 60 nm/min and the response time was 5 s. Each spectrum was the average of three scans. CD spectra were collected in Tris-HCl buffer with Na^+ or K^+ mentioned above. All the concentration of oligonucleotides and dye used for measurement was 6 μM . DNA solutions were incubated with 9E PBIC overnight at room temperature prior to the collection of spectra.

Fluorescence quantum yields

Fluorescence quantum yields (Φ) were determined by comparison with a standard solution with the following equation to calculate relative fluorescence quantum yields:⁶⁰

$$\phi_X = \phi_S \cdot \left(\frac{n_X}{n_S}\right)^2 \cdot \frac{A_S}{A_X} \cdot \frac{F_X}{F_S} \quad (1)$$

The n_X and n_S are the refractive indexes of the sample and reference, F_X and F_S are the integrated fluorescence spectra for the sample and reference respectively, and A_X and A_S are the absorbance for the sample and reference at the excitation wavelength, respectively. The standard used in this study is Rhodamine B aqueous solution with a fluorescence quantum yield of 0.97.

The stoichiometric binding analysis for dyes and c-myc

The association constants (K_a) of dye to c-myc were analyzed using Origin 8.5 (OriginLab Corporation, MA) according to the method of Benesi-Hildebrand,⁶¹ using the following equation.

$$\frac{F_\infty - F_0}{F_x - F_0} = 1 + \frac{1}{K[\text{DNA}]} \quad (2)$$

F_∞ is the fluorescence in excess DNA, in which all the dyes were bound with DNA. F_0 is the maximum fluorescence of the free dye. $[\text{DNA}]$ is the total DNA concentration and K_a is the association constant. The binding stoichiometry n (the number of the dye bound per c-myc G4) was confirmed by the job plot experiment.

Activity Inhibition experiment of G4/Hemin peroxidase

The peroxidase inhibition experiments were carried out at room temperature in Tris-HCl buffer. 8.3 μL of 60 $\mu\text{mol/L}$ c-myc was mixed to 0, 20, 50 or 100 μL of 50 $\mu\text{mol/L}$ 9E PBIC. Then Tris-HCl (10 mmol/L KCl) was added to a volume of 205 μL and kept for 2 h. And then 25 μL of 20 $\mu\text{mol/L}$ Hemin was added and kept for another 1 h. Lastly, 160 μL of 10 mmol/L ABTS and 110 μL of 10 mmol/L H_2O_2 were added. The absorption at 415 nm was recorded by UV-1900 (Beijing Purkinje General Instrument Co. Ltd.) instrument within 25 min.

NMR titration experiment

The stock solution of 9E PBIC for NMR experiments was prepared by dissolving 9E PBIC in Tris- K^+ (2.3 mM). The stock

Paper

solution of c-myc2345 was prepared by dissolving it into 0.6 mL of NMR buffer solution (10 mM $\text{KH}_2\text{PO}_4 - \text{K}_2\text{HPO}_4$, 70 mM KCl , 1 mM EDTA , 90% H_2O –10% D_2O (v/v)). NMR spectra were recorded on a Bruker Avance III 500 spectrometer, which was equipped with a 5 mm BBI probe capable of delivering z-field gradients up to 50 G cm^{-1} . The chemical shifts of the proton were referred to those of tetramethylsilane (TMS). The proton spectra were recorded using the standard pulse program p3919gp that applies 3 –9 –19 pulses with gradients for water suppression.⁶²

Molecular docking simulation

Molecular docking of the structure of 9E PBIC and c-myc G4 was carried out using the program AutoDock 4.2 Release 4.2.6. We built a homology model of the DNA (c-myc G4) based on the crystal structure of the human myc promoter (PDB ID: 2A5R)⁶³ whose sequence is “TGAGGGTGGIGAGGGTGGGAAGG”. The structure of the dye was optimized by DFTB+ software. By using Autodock program suite, the flexible docking was done by the Lamarckian genetic algorithm, searching for favorable bonding conformations of the ligand at the sites of the target DNA.

The solvent molecules were removed from the DNA 3D structure to obtain the docking grid, and the active site was defined using Auto Grid. The grid size was set to $60 \times 60 \times 60$ points with a grid spacing of 0.375 \AA . After docking process, the energy was calculated using the Tripos force field.

Results and discussion**Design of 9E PBIC**

The reported BMVC and other carbazole rivatives exhibit good selectivity to G4s, but their spectral character located at short wavelength. In this range, DNA, tissue and other organisms exhibit their special absorption and fluorescence, which may cause the overlap with those of the dyes and the errorflag occur, especially when used in vivo. And their selectivity of specific G-quadruplexes was poor. Therefore, design and synthesis of novel long-wavelength dyes with excellent specific recognition for c-myc to reduce error is a problem that can not be ignored. BMVC was chosen as the mother structure, one pyridine ring was replaced by a benzindole ring. The introduction of benzindole not only maintains the selectivity for G-quadruplexes from ds DNA and sDNA of carbazole probe but also expands the size of the π -conjugate aromatic system.

Absorption and Fluorescence Spectra of 9E PBIC

The UV-vis and fluorescent spectra in different solvents are shown in Fig. 2. The data are shown in Table 1. 9E PBIC shows an absorption maximum wavelength around 520 nm. In protic solvents, the spectra exhibited a blue shift of the λ_{max} with the increase of solvent polarity, which is the same to that of other carbazole and pyridinium compounds.⁶⁴

Analyst

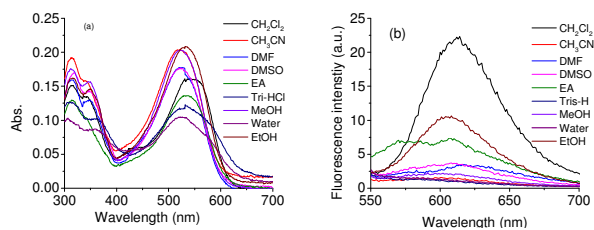


Fig. 2 Absorption (a) and fluorescence spectra (b) of the dye in different solvents

Table 1 Absorption and Fluorescence data of 9E PBIC in different solvents.

Solvent	λ_{max} (nm)	λ_{em} (nm)	Stokes shift (nm)	Φ
$\text{C}_2\text{H}_5\text{OH}$	532	601	70	0.077
CH_3OH	524	602	80	0.025
H_2O	526	603	70	0.014
CH_2Cl_2	531	614	78	0.96
EA	528	607	64	0.094
CH_3CN	521	601	80	0.021
DMF	527	618	86	0.02
DMSO	522	612	90	0.079

It is said that the absorption band was at about 520 nm and fluorescent band at 600 nm, which is longer than that of BMVC. The reason for this is the longer π -conjugate aromatic system.⁶⁵ The effect of the protic solvent polarity on λ_{max} can be illustrated by the interactions between the dye molecules and the solvents, as the interaction make ground state of dye more stable than that of excited state by forming hydrogen bond.⁶⁶⁻⁶⁸ In aprotic solvents, dipole-dipole interaction between the dye and solvents was held dominant position. The ground state of the compound has large dipole moment, when ICT occurred, the ground state was changed to the excited state with smaller dipole moment. With the increase of the solvents polarity, the energy of the ground state reduced and that of the excited state increased, which increased the energy difference and the wavelength shifted blue. The absorbing intensity enhanced with the higher polarity of the solvent because the energy of the antibonding orbital and bonding orbital of the molecular both reduced with the polarity of the solvent.

From Fig. 2, we can see that the λ_{em} shifted blue with the increasing of the dipole moment and solvent polarity in protic and aprotic solvents. In protic solvent, the λ_{em} shifted blue and fluorescence intensity evidently decreased with the increasing of the solvent polarity and is the lowest in aqueous solution. The possible reason is that the bond between the

carbazole and pyridinium was rotated and water molecules make the twist angle between the bond and bond in the molecule of the dye increase. It destroys the coplanarity of the molecule, thereby resulting in the increase of the nonradiative decay process and finally the obviously quenching occurred.⁶⁹⁻⁷² The Fluorescence quantum yield (Φ) enhanced with the decreasing solvent polarity because of the excited state of the dye is more stable than the ground state. In CH_2Cl_2 , Φ can be even up to 0.96, which is same to the standard substance Rhodamine B.

UV-vis spectra of 9E PBIC in the presence of different DNA.

In order to investigate the interaction of 9E PBIC with different DNA, the absorption spectra of 9E PBIC in the presence of twelve DNA were investigated, respectively. These DNA (Table S2) include two single-stranded DNA (s22 and s24), two duplex sequence (ds26 and d24), three parallel structure G4 sequences (c-myc, c-kit1, VEGF), two antiparallel G4 sequences (A24, 22AG in Na^+ buffer), and three mixed type G4 sequence (22AG in K^+ buffer, H24, bcl-2 2345). Among them, 22AG sequence can form different type G4 structure in different buffer condition.^{73, 74}

With the addition of 3-fold excess of preformed DNA into the dye solutions, the absorbance spectra were studied and the results were shown in Fig.3.

The absorption intensities changed when addition of DNA, while different changes occurred with the addition of different types of DNA. G4s caused an enhancement to that of the dye. In contrast, non-quadruplexes, including ss-DNA (s22 and s24), self-complementary duplex DNA (ds26), linear helical duplex DNA (d24) duplex and ct-DNA (calf thymus DNA) caused hardly enhancement under the same condition, but with only slight decrease of the absorbance. Additionally, the parallel G4s (c-myc2345, c-kit1 and VEGF) caused a stronger enhancement than those of anti-parallel G4s (A24 and 22AG in Na^+ buffer), which indicated that the compound showed a selectivity to parallel G4s. We can also see that the parallel G4s and mixed type G4s caused the appearance of a new absorption band around 425nm while ss-DNA, ds-DNA and antiparallel G4s not. Among the G4s, the parallel G4s and mix-type bcl-2 2345 caused the new band around 425 nm higher than other G4s. The appearance of a new absorption band has rarely been reported in other G4 ligands.⁴⁷ Thus, G-quadruplexes could be detected and differentiated from other forms of DNA. An absorption titration experiment was performed to further investigate the interaction between c-myc and 9E PBIC. As shown in Fig.3 the two bands enhanced upon the addition of c-myc up to 3:1 stoichiometry. Interestingly, in our work, c-myc in Na^+ can also caused a stronger enhancement which is same to that in K^+ buffer.

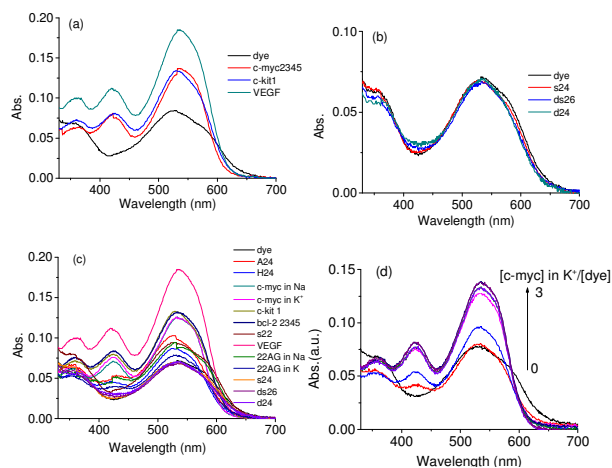


Fig. 3 (a, b, c) Absorption spectra of $6\mu\text{M}$ dye in the presence of $18\mu\text{M}$ different kinds of DNA. (d) Absorption spectra of $6\mu\text{M}$ dye in the presence of increasing amounts of c-myc G4, where the concentrations ratio of the c-myc G4 and dye are 0, 0.25, 0.5, 1, 1.5, 2, 2.5 and 3.

Fluorescence Spectra of 9E PBIC in the Presence of Different DNA.

The excitation spectra of dye ($6\mu\text{M}$) were measured at 530 nm and the fluorescence spectra and fluorometric titration curves were shown in Fig. 4

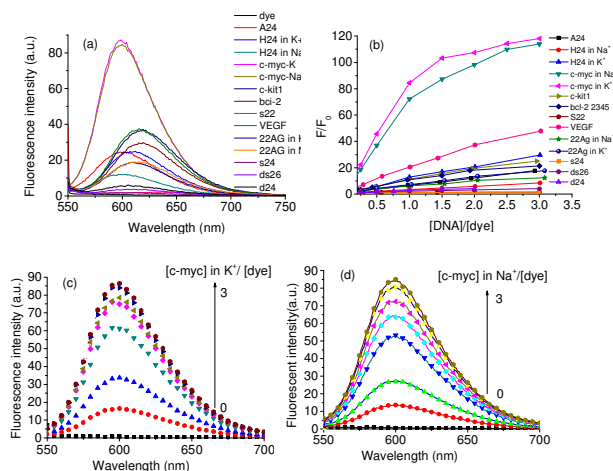


Fig. 4 a Fluorescent spectra of dye ($6\mu\text{M}$) in the absence and presence of different DNA(3eq). b Fluorometric titration curves of 9E PBIC with different DNAs. c Fluorimetric titration of 9E PBIC with c-myc in K^+ buffer (0, 0.25, 0.5, 1.0, 1.5, 2.0, 2.5, 3.0 eq.) and d Na^+ buffer, dash line represents the spectrum of dye in the absence of DNA.

Fig.4a shows the emission spectra of 9E PBIC in the presence of a variety of DNA sequences and structures. As shown in Fig.4a, no fluorescence of 9E PBIC was observed in buffer solution without DNA, very weak fluorescence was observed in the presence of ss-DNA and ds-DNA.

Weak fluorescence was observed in the presence of antiparallel G4s and mixed type G4s. Strong fluorescence was observed in the presence of parallel G4s. Very strong fluorescence was observed in the presence of c-myc in K^+ buffer. Interestingly, very strong fluorescence was also observed in the presence of in Na^+ buffer. So, it may be a light-up probe for c-myc G4.

The titration curves with different DNA revealed that the intereaction degree of fluorescence enhancement depended on the types of DNA (Fig. 4b and Fig.S1). As shown in Fig. 4b, in the presence of title twelve G4s, we observed a large fluorescence enhancement was induced by parallel G4s and weaker fluorescence enhancement by mixed parallel/antiparallel G4s relative 9E PBIC alone, respectively. Very weak fluorescence enhancement was observed when ss-DNA and ds-DNA added, indicating their poor binding affinity toward ss-DNA and ds-DNA. These results indicate that the 9E PBIC can be used as a fluorescent probe with good sensitive and excellent selectivity toward parallel c-myc G4 over other G4s, ss-DNA and ds-DNA.

Fluorescence titration with excitation at 530 nm was carried out to study the response of the dye to different types of DNA. As shown in Figure 4c and 4d, with the addition of c-myc, the fluorescence intensity was remarkably enhanced up to 118-fold in K^+ buffer and 114-fold in Na^+ buffer at saturation. The sensitivity of the 9E PBIC as a light-up fluorescent probe was investigated by fluorimetric titration of 9E PBIC with c-myc. It can be seen that there is a good linear relationship between the concentration (1.5–6.0 μM) and fluorescence intensity ($R^2=0.9996$). Interestingly, there is also a same good linear relationship in Na^+ buffer ($R^2=0.9998$) (Fig.S2). The limit of detection was estimated to be 0.0136 μM according to the 3σ criteria (defined as $3\sigma/\text{slope}$, where σ is the standard deviation of the blank solution).

The titration curves were further fitted to an independent-site model (eq 1, Materials and Methods); the binding affinity and stoichiometry between 9E PBIC and c-myc G4 were calculated. A 1:1 binding model was fitted to the titration data of c-myc (Fig. 4b) and was further confirmed by the job plot analysis (Fig.S3). The apparent binding constants (K_a) between 9E PBIC and c-myc G4s are almost the same in Na^+ and K^+ buffer (1.14×10^5 and 1.36×10^5 respectively).

Furthermore, the recognizing ability of 9E PBIC to c-myc over duplex DNAs shows that the probe exhibits a high fluorescence selectivity (47 folds, at a 3:1 ratio of [c-myc]:[dye]). Compared with the known fluorescent probes, such as PDC-M-TO (8 folds), dinuclear ruthenium complex (15 folds) showed a little selectivity over duplex DNAs. Macrocyclic hexaoxazole dimmers, aminosugar-bisbenzimidazoles and

others showed only a little or no enhancement when interact with the specific G-quadruplex.

The response of 9E PBIC probe to c-myc G4 is in real time. The time-dependent fluorescence measurement was done once the 9E PBIC was injected in and the result was shown in Fig.5. The fluorescent intensity exhibited a sharp increase once c-myc was added in and reached the maximum value within 30s according to the time appeared in the inflection points, meaning that the probe is of an excellent performance in quick measurement.

Effect of 9E PBIC on CD spectra of c-myc G4

The effect of the dye on the conformation of G4s was investigated by measuring the CD spectra of G4s in the absence and presence of the dye (Fig.6).

In the absence of the dye, the CD spectra of the parallel G4s showed a characteristic negative peak at 242 nm and a positive peak at 263 nm. The antiparallel G4s exhibited two positive peaks at 252 nm and 290 nm, respectively. The mixed-type G4s showed a positive peak at 287 nm.

The addition of 9E PBIC to G4s solutions only make the characteristic CD peaks increased slightly, indicating that the dye did not cause significant conformational transition of the dye could interact with c-myc both in Na^+ and K^+ buffer.

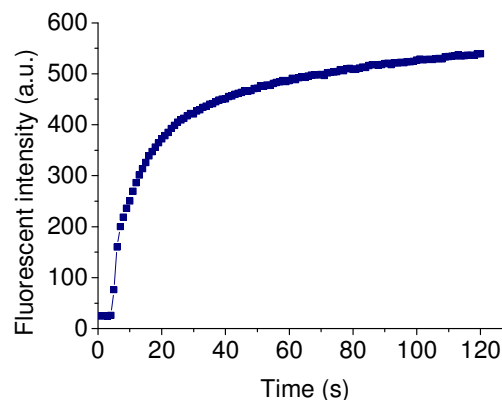


Fig. 5 The fluorescence intensity at 530 nm of 9E PBIC with time after addition of c-myc.

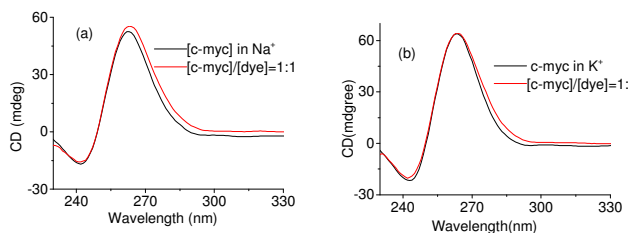


Fig. 6 CD spectra of c-myc G4 in Na^+ buffer and K^+ buffer with the dye at [DNA]/[dye]=1:1.

Determination of Binding Model

The main binding modes of organic ligand with G4s are grooves and end-stacking binding, especially with parallel G4s⁷⁵. In order to prove the title compound binding to the parallel c-myc G4 mainly by end-stacking, an inhibition experiment on the G4/hemin peroxidase activity by the compound was performed. Hemin is considered to be bound to G4 DNA by end-stacking and consequently exhibits catalytic activity on the oxidation of ABTS²⁻ by H₂O₂.⁷⁶ Candidate ligands having the same sites will compete with hemin for G4 binding, resulting in the decrease rate of catalytic oxidation of G4/hemin peroxidase. As we expected, with the addition of the title compound, the absorbance at 415 nm (the oxidized product of ABTS²⁻) showed a strong restraint, indicating that the compound competed with hemin and inhibited the activity of c-myc/hemin peroxidases (Fig. 7). This result proved that the compound bound with c-myc G4 had the same mode with hemin by the end-stacking mode

In order to further understand the binding model, ¹H NMR titration experiments between the dye and c-myc 2345 were carried out. The c-myc 2345 is a wild-type sequence, which is predicted to restrict the mixture of loop isomers to a parallel G-quadruplex structure⁷⁷. The guanine imino proton signals of c-myc 2345 are well visible in the low field regions (about 10-12 ppm)⁷⁸ as shown in Fig.8.

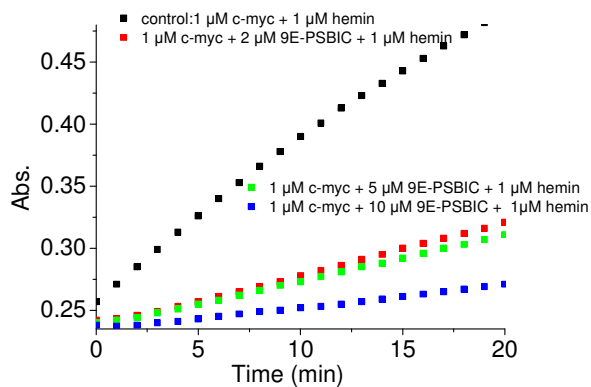


Fig. 7 Inhibition activity of 9E PBIC on the peroxidase activity of G4/hemin complexes. The curves represent the change of the product concentration of G4/hemin peroxidase within 20 min using the G4/hemin reaction without 9E PBIC as the control.

9E PBIC : c- myc 2345

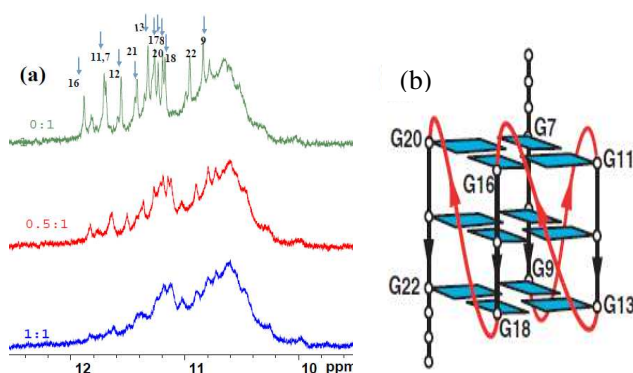


Fig. 8 The ¹H-NMR titration spectra of 200 μM c-myc2345 with different concentrations of 9E PBIC in 0.6 mL PBS (10 mM KH₂PO₄-K₂HPO₄, 70 mM KCl, 1 mM EDTA, pH 7.4 (H₂O-D₂O 9/1, v/v))(left) and the NMR-based folding topologies of the DNA (right).The blue arrows show the signals that changed.

Adding 9E PBIC to c-myc 2345 (from 0:1 to 1:1) results in a change of the imino protons. ¹H NMR titration results demonstrated that in the presence of 9E PBIC, the protons exchange occurred. The exchangeable protons in the chemical shift range characteristic of guanine quarter imino protons as well as exchangeable protons from the loop residues. The results indicating that 9E PBIC could label the c-myc 2345 G4.

In order to better understand the interactions between 9E PBIC and parallel G4 c-myc2345, a molecular docking study was carried out using Sybyl X 1.1. A crystal structure of 9E PBIC with monomeric parallel G4 complex from PDB (Pu24I, code 2A5R) was chosen for the docking (Fig. 9 and Fig.S4).

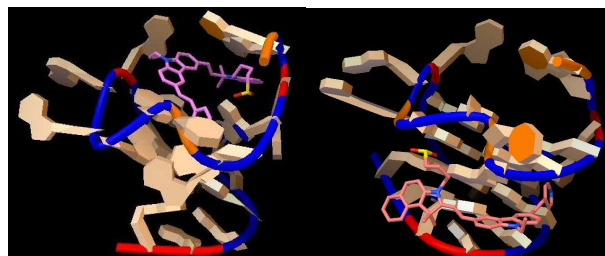


Fig. 9 Binding model of 9E PBIC to c-myc G4 (PDB: 2A5R) by molecular docking. (a) side view of BPBC stacking on the surface of G-quartet. (b) Side view of 9E PBIC binding to the groove. 9E PBIC is shown in "sticks" model colored by atom

Paper

Analyst

type (pink-red-yellow-blue). Propeller-shaped G4 molecule is represented in a ribbon form (muddy-red-blue-orange)

As shown in Fig. 9 and Fig.S4, when the dye stacks on the 5'-terminal G-quartet, the dye is twisted to form a quasi-coplanar conformation for maximizing the π - π interaction. Some energy data are shown below. The binding energy of end-stacking interaction mode is (-11.2 Kcal/mol) lower than that of the groove binding interactions mode (-8.68Kcal/mol), suggesting that the end-stacking mode is more stable and favored over the groove binding mode.

To the end-stacking interaction mode, the final intermolecular energy (1) is -14.00 kcal/mol, including the addition energy of vdW, Hbond and desolv is -13.95 kcal/mol and electrostatic energy is -0.05 kcal/mol. Final total internal energy (2) is -2.06 kcal/mol. Torsional free energy (3) is +2.98 kcal/mol and unbound system's energy (4) is -2.06 kcal/mol same which is to that of (2). Finally, the estimated free energy of binding is equal to (1)+(2)+(3)-(4), which is -11.02 kcal/mol.

Discussion

9E PBIC contains a benzindole ring substituted carbazole planar core, which is designed from the cyanine dye and BMCVC (a disubstituted carbazole derivative). Compared with the cyanine dye and BMVC, 9E PBIC exhibited good selectivity to specific c-myc G4 over other G4s, ds DNA and sDNA forms. It may be due to its larger size of the planar core.

Conclusions

In summary, a novel compound 9E PBIC with longer emission wavelength based on BMVC was designed and synthesized as a c-myc G4 targeting probe. Fluorescent spectra showed that there was almost no fluorescence in aqueous buffer, but a large fluorescence enhancement when bond with parallel G4s, especially with c-myc G4. For antiparallel and mixed parallel/antiparallel types G4s, the fluorescence enhancement was much smaller and for ss-DNA and ds-DNA, there is almost no enhancement. The results show that the compound can distinguish c-myc G4s from other DNA forms. The hemin/G4 peroxidase inhibition experiment and molecular docking studies suggested that the dye interact with parallel c-myc G-quadruplex by end-stacking mode. It is said that it can be a potential light up probe for targeting c-myc G-quadruplex, which gives a clue to explore new dyes to be used as specific quadruplex probe for diagnostic, therapeutic and biosensor.

Acknowledgements

The present study was financially supported by the National Natural Science Foundation of China (grant no. 51178289, 11447222) and Technology Development Foundation Plan Project of Tianjin Colleges (20130505).

Notes and references

- 1 Burge, G. N. Parkinson, P. Hazel, A. K. Todd and S. Neidle, *Nucleic Acids Res.*, 2006, **34**, 5402–5415.
- 2 M. L. Bochman, K. Paeschke and V. A. Zakian, *Nat. Rev. Genet.*, 2012, **13**, 770–780.
- 3 A. K. Todd, M. Johnston and S. Neidle, *Nucleic Acids Res.*, 2005, **33**, 2901–2907.
- 4 J. L. Huppert and S. Balasubramanian, *Nucleic Acids Res.*, 2005, **33**, 2908–2916.
- 5 K. Cao, P. Ryvkin and F. B. Johnson, *Methods*, 2012, **57**, 3–10.
- 6 G. N. Parkinson, M. P. Lee and S. Neidle, *Nature*, 2002, **417**, 876–880.
- 7 A. Siddiqui-Jain, C. L. Grand, D. J. Bearss, and L. H. Hurley, *Proc. Natl. Acad. Sci. U. S. A.*, 2002, **99**, 11593–11598.
- 8 T. S. Dexheimer, D. Sun and L. H. Hurley, *J. Am. Chem. Soc.*, 2006, **128**, 5404–5415.
- 9 M. J. Morris, Y. Negishi, C. Pazsint, J. D. Schonhoft and S. Basu, *J. Am. Chem. Soc.*, 2010, **132**, 17831–17839.
- 10 R. I. Mathad, E. Hatzakis, J. Dai and D. Yang, *Nucleic Acids Res.*, 2011, **39**, 9023–9033.
- 11 G. Biffi, D. Tannahill, J. Mc Cafferty and S. Balasubramanian, *Nat. Chem.*, 2013, **5**, 182–186.
- 12 S. Balasubramanian, L. H. Hurley and S. Neidle, *Nat. Rev. Drug Discov.*, 2011, **10**, 261–275.
- 13 A. De. Cian, L. Lacroix, C. Douarre, N. Temime-Smaali, C. Trentesaux, J. F. Riou and J. L. Mergny, *Biochimie*, 2008, **90**, 131–155.
- 14 W. Zhou, N. J. Brand and L. Ying, *J. Cardiovasc. Transl. Res.*, 2011, **4**, 256–270.
- 15 J. D. Schonhoft, R. Bajracharya, S. Dhakal, Z. Yu, H. Mao and S. Basu, *Nucleic Acids Res.*, 2009, **37**, 3310–3320.
- 16 C. Chen, L. Zhou, J. Geng, J. Ren and X. Qu, *Small*, 2013, **9**, 2653–2653.
- 17 L. Zheng, X. Wang, J. L. Zhang and W. Li, *Prog. Chem.*, 2011, **23**, 974–982.
- 18 C. Wang, G. Jia, J. Zhou, Y. Li, Y. Liu, S. Lu and C. Li, *Angew. Chem. Int. Ed.*, 2012, **51**, 9352–9355.
- 19 S. N. Georgiades, N. H. Abd Karim, K. Suntharalingam and R. Vilar, *Angew. Chem. Int. Ed.*, 2010, **49**, 4020–4034.
- 20 J. Alzeer, B. R. Vummidi, P. J. C. Roth, and N. W. Luedtke, *Angew. Chem. Int. Ed.*, 2009, **48**, 9362–9365.
- 21 A. C. Bhasikuttan, J. Mohanty and H. Pal, *Angew. Chem. Int. Ed.*, 2007, **46**, 9305–9307.
- 22 D. M. Kong, Y. E. Ma, J. Wu and H. X. Shen, *Chem.–Eur. J.*, 2009, **15**, 901–909.
- 23 M. P. Teulade-Fichou, C. Carrasco, L. Guittat, C. Bailly, P. Alberti, J. L. Mergny, A. David, J. M. Lehn and W. D. Wilson, *J. Am. Chem. Soc.*, 2003, **125**, 4732–4740.
- 24 P. Yang, A. De Cian, M. P. Teulade-Fichou, Mergny and J. L. Monchaud, *Angew. Chem. Int. Ed.*, 2009, **48**, 2188–2191.
- 25 H. Arthanari, S. Basu, T. L. Kawano, and P. H. Bolton, *Nucleic Acids Res.*, 1998, **26**, 3724–3728.
- 26 J. H. Guo, L. N. Zhu, D. M. Kong, and H. X. Shen, *Talanta*, 2009, **80**, 607–613.
- 27 J. W. Yan, W. J. Ye, S. B. Chen, W. B. Wu, J. Q. Hou, T. M. Ou, J. H. Tan, D. Li, L. Q. Gu and Z. S. Huang, *Anal. Chem.*, 2012, **84**, 6288–6292.a
- 28 T. Li, E. K. Wang, and S. J. Dong, *Anal. Chem.*, 2010, **82**, 7576–7580.
- 29 J. Mohanty, N. Barooah, V. Dhamodharan, S. Harikrishna, P. I. Pradeepkumar, and A. C. Bhasikuttan, *J. Am. Chem. Soc.*, 2013, **135**, 367–376.
- 30 G. Sivaraman, T. Anand and D. Chellappa, *Chem. Plus. Chem.*, 2014, **79**, 1761–1766.

Analyst

Paper

- 1
2
3
4
5
6
7
8
9
10
11
12
13
14
15
16
17
18
19
20
21
22
23
24
25
26
27
28
29
30
31
32
33
34
35
36
37
38
39
40
41
42
43
44
45
46
47
48
49
50
51
52
53
54
55
56
57
58
59
- 31 A. Laguerre, L. Stefan, M. Larrouy, D. Genest, J. Novotna, M. Pirrotta and D. Monchaud, *J. Am. Chem. Soc.*, 2014, **136**, 12406–12414.
- 32 C. V. Dang, L. M. S. Resar, E. Emison, S. Kim, Q. Li, J. E. Prescott, D. Woney and K. Zeller, *Exp. Cell Res.*, 1999, **253**, 63.
- 33 T. M. Ou, Y. J. Lu, C. Zhang, Z. S. Huang, X. D. Wang, J. H. Tan, Y. Chen, D. L. Ma, K. Y. Wong, J. C. O. Tang, A. S. C. Chan and L. Q. Gu, *J. Med. Chem.*, 2007, **50**, 1465–1474.
- 34 V. Gonzalez and L. H. Hurley, *Annu. Rev. Pharmacol. Toxicol.*, 2010, **50**, 111–129.
- 35 H.Z. He, K.H. Leung, W. Wang, D.S. Chan, C.H. Leung, and D.L. Ma, *Chem. Commun.*, 2014, **50**, 5313–5315.
- 36 D. L. Ma, H. Z. He, K. H. Leung, H. J. Zhong, D.S. Chan, and C.H. Leung, *Chem. Soc. Rev.*, 2013, **42**, 3427–3440.
- 37 H. Z. He, D.S. Chan, C.H. Leung, and D. L. Ma, *Nucleic Acids Res.*, 2013, **41**, 4345–4359.
- 38 J. Q. Hou, S. B. Chen, L. P. Zan, T. M. Ou, J. H. Tan, L. G. Luyt and Z. S. Huang, *Chem. Commun.*, 2015, **51**, 198–201.
- 39 K. R. J. Thomas, J. T. Lin, Y. T. Tao, and C. K. Ko, *J. Am. Chem. Soc.*, 2001, **123**, 9401–9411.
- 40 K. Brunner, A.V. Dijken, H. Bomer, J. J. A. M. Bastlaansen, N. M. M. Kiggen and B. M. W. Langeveld, *J. Am. Chem. Soc.*, 2004, **126**, 6035–6042.
- 41 S. M. Song, D. Ju, J. F. Li, D. X. Li, Y. L. Wei, C. Dong, P. H. Lin and S. M. Shuang, *Talanta*, 2009, **77**, 1707–1714.
- 42 H. X. Shao, X. P. Chen, Z. X. Wang, and P. Lu, *J. Lumin.*, 2007, **127**:349–354.
- 43 A. Casey, R. S. Ashraf, Z. P. Fei and M. Heene, *Macromolecules*, 2014, **47**, 2279–2288.
- 44 C. C. Chang, J. Y. Wu, C. W. Chien, W. S. Wu, H. Liu, C. C. Kang, L. J. Yu and T. C. Chang, *Anal. Chem.*, 2003, **75**, 6177–6183.
- 45 C. C. Chang, I. C. Kuo, I. F. Ling, C. T. Chen, H. C. Chen, P. J. Lou, J. J. Lin, and T. C. Chang, *Anal. Chem.*, 2004, **76**, 4490–4494.
- 46 Y. L. Tsai, Z. F. Wang, W. W. Chen and T. C. Chang, *Nucleic Acids Research*, 2011, **39**, 114.
- 47 B. Jin, X. Zhang, W. Zheng, X. J. Liu, C. Qi, F. Y. Wang and D. H. Shangguan, *Anal. Chem.*, 2014, **86**, 943 – 952
- 48 Maji B., K. Kumar, K. Muniyappa and S. Bhattacharya. *Org. Biomol. Chem.*, 2015, DOI: 10.1039/C5OB00675A
- 49 X. Xie, B. Choi, E. Largy, R. Guillot, A. Granzhan and M.-P. Teulade-Fichou, *Chem. Eur. J.*, 2013, **19**, 1214– 1226.
- 50 L. Yuan, W. Lin, K. Zheng, L. He and W. Huang, *Chem. Soc. Rev.*, 2013, **42**, 622.
- 51 Y. J. Lu, S. C. Yan, F. Y. Chan, L. Z., W. H. Chung, W. L. Wong, B. Qiu, N. Sun, P. H. Chan, Z. S. Huang, L. Q. Gu and Kwok-Yin Wong. *Chem. Commun.*, 2011, **47**, 4 971–4973.
- 52 R. Nanjunda, E. A. Owens, L. Mickelson, S. Alyabyev, N. Kilpatrick, S. M. Wang, M. Henary and W. D. Wilson. *Bioorganic & Medicinal Chemistry*, 2012, **20**, 7002–7011.
- 53 H. Ihmels and L. Thomas, *Org. Biomol. Chem.*, 2013, **11**, 480–487.
- 54 H. X. Sun, J. F. Xiang, W. Gai, Y. Liu, A. J. Guan, Q. F. Yang, Q. Li, Q. Shang, H. Su, Y. L. Tang and G. Z. Xu, *Chem. Commun.*, 2013, **49**, 4510–4512.
- 55 W. Gai, Q. F. Yang, J. F. Xiang, W. Jiang, Q. Li, H. X. Sun, J. Guan, Q. Shang, H. Zhang and Y. L. Tang, *Nucleic Acids Res.*, 2013, **41**, 2709–2722.
- 56 Y. Q. Chen, S. Y. Yan, L. B. Yuan, Y. M. Zhou, Y. Y. Song, H. Xiao, X. C. Weng and X. Zhou, *Org. Chem. Front.*, 2014, **1**, 267–270
- 57 H. P. Shi, J. X. Dai, L. W. Shi, L. Xu, Z. B. Zhou and Y. Zhang, *Spectrochimica Acta Part A.*, 2012, **93**, 19– 25.
- 58 Z. G. Yang, N. Zhao, Y. M. Sun, F. Miao, Y. Liu, X. Liu, Y. H. Zhang, W. T. Ai, G. F. Song, X. Y. Shen, X. Q. Yu, J. Z. Sun and W. Y. Wong. *Chem. Commun.*, 2012, **48**, 3442–3444.
- 59 H. Langhals, A. Varja, P. Laubichler, M. Kernt, K. H. Eibl and C. Haritoglou, *J. Med. Chem.*, 2011, **54**, 3903–3925.
- 60 H. A. Benesi and J. H. Hildebrand, *J. Am. Chem. Soc.*, 1949, **71**, 2703–2707
- 61 G. A. Crosby and J. N. Demas, *J. Phys. Chem.*, 1971, **75**, 991–1024.
- 62 M. Piotto, V. Saudek and V. Sklenar, *J. Biomol. NMR*, 1992, **2**, 661–665.
- 63 A. T. Phan, V. Kuryavyi, H. Y. Gaw and D. J. Patel. *Nat. Chem. Biol.* 2005, **1**, 167–173.
- 64 H. Y. Woo, J. W. Hong, B. Liu, A. Mikhailovsky, D. Korystov and G. C. Bazan, *J. Am. Chem. Soc.* 2005, **127**, 820–821.
- 65 C. C. Chang, J. F. Chu and H. H. Kuo, *J. Lumin.*, 2006, **119**, 84–90.
- 66 A. Mishra, R. K. Behera, P. K. Behera and B. K. Mishra, *Chem. Rev.* 2000, **100**, 1973–2011.
- 67 B. Song, Q. Zhang, W. H. Ma, X. J. Peng, X. M. Fu and B. S. Wang, *Dyes and Pigments*, 2009, **82**, 396–400.
- 68 U. Narang, C. F. Zhao, J. D. Bhawalkar, F.V Bright and P.N. Prasad, *J Phys.Chem.*, 1996, **100**, 4521–4525.
- 69 W. Rettig and R. Lapouyade, *Top. Fluoresc. Spectrosc.*, 1994, **4**, 109–149.
- 70 M. C. Castex, C. Olivero, G. Pichler, D. Ades, E. Cloutet and A. Siove, *Synthetic Met.*, 2001, **122**, 59–61.
- 71 D. Ade's, V. Boueard, E. Cloutet, A. Siove1, C. Olivero, M. C. Castex and G. Pichler, *J Appl. Phys.*, 2000, **57**, 7290–7293.
- 72 B. Strehmel, A. M. Sarker, J. H. MalPert, V. Strehmel, H. Seifert and D. C. Neckers, *J. Am. Chem. Soc.*, 1999, **121**, 1222–1236.
- 73 X. H. Cheng, X. J. Liu, T. Bing, R. Zhao, S. X. Xiong and Shangguan, D. H. *Biopolymers*, 2009, **91**, 874 883.
- 74 J. X. Dai, M. Carver, L. H. Hurley and D. Z. Yang, *J. Am. Chem. Soc.* 2011, **133**, 17673–17680.
- 75 D. R. Boer, A. Canals and M. Coll, *Dalton Trans.*, 2009, **21**, 399–414.
- 76 L. J. Yu, Q. F. Yang, J. F. Xiang, H. X. Sun, L. X. Wang, Q. Li, A. J. Fuan and Y. L. Tang, *Analyst*, 2015, **140**, 1637–1646.
- 77 A. T. Phan, Y. S. Modi and D. J. Patel, *J. Am. Chem. Soc.* 2004, **126**, 8710–8716
- 78 M. Y. Tian, X. F. Zhang, Y. Li, Y. Ju, J. F. Xiang, C. Q. Zhao and Y. L. Tang, *Nucleosides, Nucleotides and Nucleic Acids*, 2010, **29**, 190–199.